Journal of Orthopaedic Surgery and Research

RESEARCH

Open Access

Dichotomitin promotes osteoblast differentiation and improves osteoporosis by inhibiting oxidative stress

Meichun Han[1,2†], Weibin Du[1†], Lei Zhang[3†], Zhenwei Wang[1,2], Shengqiang Fang[1,2], Yang Zheng[1,4*] and Renfu Quan[1*]

Abstract

Objective Osteoporosis is a systemic disease with high morbidity and significant adverse effects. Increasing evidence supports the close relationship between oxidative stress and osteoporosis, suggesting that treatment with antioxidants may be a viable approach. This study evaluated the antioxidant properties of dichotomitin (DH) and its potential protective effects against osteoporosis.

Methods SD rats were divided into three groups: Sham, OVX, and OVX + DH (5 mg/kg, intraperitoneal injection twice weekly). After three months, blood samples, femurs, and tibiae were collected for analysis. Micro-CT evaluated the femoral, while histological examination assessed tibial tissues. Serum osteogenic biochemical markers were measured. In vitro, osteogenic differentiation was induced with varying concentrations of DH, followed by ALP and ARS staining. RT-qPCR and western blot were used to assess the expression of osteogenesis-related genes and proteins. Additionally, an oxidative stress cell model was established, dividing cells into control, H_2O_2-treated, and H_2O_2 + DH-treated groups. Expression of oxidative stress-related genes and proteins was assessed using real-time quantitative PCR and western blotting.

Results Micro-CT and histological staining revealed decreased and disrupted bone trabeculae in the OVX group, whereas the DH-treated group exhibited enhanced bone trabecular area and structure compared to the OVX group. In vitro studies showed that DH enhanced ALP activity and elevated expression of RUNX2, OPN, OCN, SOD1, and SOD2.

Conclusion DH has the potential to enhance osteoblast differentiation and alleviate osteoporosis through the attenuation of oxidative stress.

Keywords Oxidative stress, Osteoporosis, Dichotomitin, Osteoblast, Micro-CT

†Meichun Han, Weibin Du and Lei Zhang contributed equally to this work.

*Correspondence:
Yang Zheng
0623112@zju.edu.cn
Renfu Quan
quanrenfu@zcmu.edu.cn

[1]Research Institute of Orthopedics, The Affiliated Jiangnan Hospital of Zhejiang Chinese Medical University, Hangzhou, China
[2]Zhejiang Chinese Medical University, Hangzhou, China
[3]Xuzhou Municipal Hospital Affiliated to Xuzhou Medical University (Xuzhou First People's Hospital), Xuzhou, China
[4]Department of Orthopaedic Surgery, Sir Run Run Shaw Hospital, Zhejiang University School of Medicine, Hangzhou, China

Introduction

Osteoporosis (OP) is marked by greater bone resorption than formation, main to reduced bone mass, weakened bone strength, and deteriorated bone microarchitecture [1]. This condition heightens bone fragility and fracture susceptibility, leading to substantial health risks and economic burdens, especially in older adults [2, 3]. Identifying high-risk fracture groups and providing them with appropriate treatment options are crucial steps in managing this disease. Current medications like bisphosphonates, denosumab, and estrogens are associated with significant drawbacks, including severe side effects, high costs, and prolonged treatment regimens, which frequently result in poor patient compliance [4, 5]. Therefore, there is a pressing urgent want to improve anti-osteoporosis capsules that offer improved efficacy and fewer adverse effects.

Oxidative stress takes place when an equilibrium between oxidative and antioxidant processes, leads to an oxidation-prone state within an organism [6]. Immoderate reactive oxygen species (ROS) induced by oxidative stress can impair redox-sensitive transcription factors, compromising mitochondrial and DNA integrity. Consequently, the cellular DNA repair mechanisms may become less effective in addressing oxidative damage, leading to DNA damage accumulation that can trigger apoptosis (programmed cell death) or necrosis, further causing tissue damage [7, 8]. Growing evidence indicates that excessive ROS production negatively impacts bone metabolism and contributes to osteoporosis [9, 10]. Oxidative stress performs an imperative function in the onset and development of osteoporosis. Elevated oxidative stress now not solely causes significant apoptosis of primary osteoblasts but additionally inhibits osteogenic differentiation [11–13]. Therefore, mitigating oxidative stress could promote osteoblast proliferation, although the specific mechanisms require further investigation.

Dichotomitin (DH) is an isoflavonoid derived from Belamcanda Rhizoma. Belamcanda Rhizoma has been mentioned to possess a variety of beneficial outcomes along with anti-inflammatory, adhesion-inducing, antimutagenic, anti-angiogenic, chemosensory, and antimicrobial properties. It also acts to prevent biomolecule over-oxidation through several antioxidant mechanisms such as reducing transition metal ions, inhibiting lipid peroxidation, and scavenging free radicals [14, 15]. The main active components of Belamcanda Rhizoma extracts include isoflavones like tectoridin, tectorigenin, dichotomitin, and iristectorigein A. Both tectoridin and tectorigenin exhibit antioxidant effects [16, 17].

Therefore, it is plausible that DH also possesses antioxidant properties. In this study, we aimed to confirm this speculation and explore whether DH promotes osteoblast differentiation to mitigate osteoporosis. This research marks the first discovery of DH's potential therapeutic role in osteoporosis treatment, offering a possible strategy for addressing this condition.

Materials and methods

Animals

Twelve wholesome female SFP-grade SD rats, weighing 220±20 g, had been provided through the Experimental Centre of Zhejiang Chinese Medical University. The rats were housed at the Experimental Centre under controlled conditions: room temperature 21℃~25℃, humidity 55%~70%, with free admission to water and general pellet feed. All procedures adhered to the 'Regulations on the Administration of Laboratory Animals' of the People's Republic of China. The experimental protocol was approved by the Ethics Committee of Zhejiang Chinese Medical University (IACUC-20210517-05).

Chemical reagents

Dichotomitin (160 mg) was purchased from Med Chem Express, Inc.

Animal groups

The rats were randomly assigned to three groups (every consisting of four animals): Sham, OVX, and OVX+DH group. The OVX+DH group received intraperitoneal injections of DH (5 mg/kg) twice a week. After three months, the rats were euthanized with CO_2 overdose. Then the abdominal aortic blood was centrifuged, and the serum was collected. Bilateral femurs were harvested, processed, and fixed for analysis.

Animal model

Bilateral ovariectomy (OVX) was performed to induce an osteoporosis (OP) model in rats. They were first anesthetized with sodium pentobarbital (30 mg/kg intraperitoneally). Then skin over the mid-spine was shaved and sterilized, and 3 cm longitudinal incisions were made on both sides of the spine. The ovaries were removed after identifying the surrounding fat tissue, while in the sham group, the ovaries remained intact. The remaining tissue was returned to its original position, and the incision was sutured. Postoperatively, each rat received an intramuscular injection of 80,000 units of penicillin sodium.

Micro-CT Assessment

The rat femurs were harvested, and the soft tissues at the distal ends were excised, fixed in paraformaldehyde for 48 h, and then stored in a 75% ethanol solution. The distal femur was scanned using Micro-CT (Skyscan 1176, Bruker-microCT, Kontich, Belgium) with the following scanning parameters: resolution 8.73 μm, voltage 42 kV, current 555 μA, and exposure time 786 ms. Three-dimensional images were generated using CTvox software (v3.0,

SkyScan) to visualize bone microstructural changes. The trabecular bone volume/tissue volume ratio (BV/TV), bone surface/volume ratio (BS/BV), trabecular number (Tb.N), trabecular bone separation (Tb.Sp), and trabecular thickness (Tb.Th) were then calculated.

Enzyme-linked immunosorbent assays (ELISA)

The serum was retrieved at -80 °C (for the collection method, see Sect. 2.3). ALP, OCN, and OPN levels were measured using their respective ELISA kits (Yuxiang, Zhejiang, China) according to the manufacturer's instructions. Briefly, standard and sample wells were prepared. In the standard wells, 50 μL of standard solutions with concentrations of 0, 3, 6, 12, 24, and 48 ng/mL were added. For the sample wells, 10 μL of the test sample was first added, followed by 40 μL of sample diluent. In both the standard and sample wells, 100 μL of HRP-conjugated detection antibody was added. The wells were sealed with adhesive film and incubated at 37 °C for 60 min. After discarding the liquid, the wells were blotted dry with filter paper. Wash buffer was then added to each well, left for 1 min, discarded, and the wells were blotted dry again. This washing procedure was repeated five times. Next, 50 μL of substrate A and 50 μL of substrate B were added to each well, and the plates were incubated in the dark at 37 °C for 15 min. Finally, 50 μL of stop solution was added to each well, and the absorbance (OD) of each well was measured at 450 nm within 15 min.

Histopathological analysis

The tibia was fixed, decalcified with EDTA for 4 weeks, dehydrated, and embedded. The specimen was sectioned into 5 μm. Sections were stained with HE and subjected to immunohistochemical staining for TRAP, OPN, and MMP9. Analysis was conducted using Image-Pro Plus 6.0 software.

Cell culture

The HS-5 cell line was maintained in DMEM/F-12 medium with 10% fetal bovine serum, 1% glutamine, and 1% antibiotic solution at 37 °C and 5% CO_2. Cells at 70–80% confluence were trypsinized with TrypLE™ Select at a 1:3 ratio for passaging. HS-5 cells are human bone marrow stromal cells derived from the stroma of a 30-year-old Caucasian male patient. These cells are isolated from bone marrow tissue, show fibroblast-like morphology, and have osteogenic differentiation capacity. They are adherent and represent a transformed cell line. The information referenced in HS-5 (CL-0798) was kindly provided by Wuhan Pricella Biotechnology Co., Ltd.

Cell proliferation assay

To evaluate the impact of DH on cell proliferation, a CCK-8 assay was performed. HS-5 were cultured in 96-well plates and exposed to media with DH concentrations of 0 μM, 0.5 μM, 1.0 μM, 1.5 μM, and 2.0 μM. At specified intervals, 10 μL of CCK-8 was once delivered to every nicely and then placed in an incubator for 1–2 h. Absorbance at 450 nm was measured with the usage of a microplate reader, and OD values had been recorded. Experiments were conducted at 24, 48, 72, and 96 h post-treatment.

ALP staining

HS-5 were seeded in 24-well plates and induced for osteogenesis at 70–80% confluence. The control group received only the osteogenic induction solution, whereas the experimental group received the osteogenic induction solution with DH concentrations of 0.5 μM, 1.0 μM, 1.5 μM, and 2.0 μM. Staining was performed on the 7th day using the Alkaline Phosphatase BCIP/NBT Chromogenic Kit.

ALP activity assay

On the 7th of osteogenic differentiation, the cells were lysed and centrifuged to obtain the supernatant. The activity was then measured following the guidelines furnished with the ALP assay kit. Each group was tested with a minimum of three replicates to ensure reliable comparisons.

ARS staining

Cells were stained on day 21 of osteogenic differentiation following the steps in the Osteoblast Mineralized Nodule Staining Kit. The medium was removed, and the cells were washed thrice with PBS, fixed for 30 min, washed thrice with ddH_2O, and stained with ARS solution for 30 min.

Determination of ARS activity

After ARS staining, images of the plates were captured and then allowed to dry.1 mL of 10% cetylpyridinium chloride was then brought to the wells and shaken on a horizontal shaker for 30 min. 200 μL aliquot from every nicely used to be transferred to a 96-well plate and measured the 570 nm absorbance. The data were quantitatively analyzed using GraphPad Prism 9.

Construction and measurement of cellular model of oxidative stress

Upon reaching 70–80% confluence, cells were treated with 100 μM H_2O_2 for 1 h. Then H_2O_2 was removed and added serum-free medium containing 10 μM 2,7-dichlorofluorescein diacetate (DCFH-DA) and then placed in an incubator for 20 min. Finally, the cells were washed

thrice with serum-free culture medium and observed under a fluorescence microscope.

15 RT-qPCR

RNA was extracted using the RNA-Quick Purification Kit. The concentration and purity of the RNA solution were determined utilizing a Micro Nucleic Acid and Protein Analyser. The cDNA was synthesized following the cDNA Synthesis Kit instructions. The qPCR reaction mixture was prepared following the guidelines of the 2X PowerUp SYBR Green Master Mix. The amplification and melting curves were confirmed at the end of the procedure. GAPDH was used as an internal control, and the gene expression between groups was normalized and calculated by the 2-ΔΔCt method. Primer sequences are listed in Table 1.

Western blot

Appropriate volumes of RIPA lysate were combined with 100X protein phosphatase inhibitor complex I and 100 mM PMSF to achieve a 1X concentration. The mixture was pipetted repeatedly to ensure thorough mixing. Cell lysates were added at a ratio of 300 μL lysate per well. The mixture was re-pipetted to ensure complete cell lysis and then put on ice for 5–10 min. Then centrifuged at 12,000 rpm for 10 min. Removed the supernatant to a new centrifuge tube, and protein concentration was measured by the BCA method. The protein sample buffer was added to the supernatant, followed by boiling the samples. Electrophoresis was followed by membrane transfer via the wet transfer method. The membranes were blocked, incubated with antibodies, and washed, and the gray values were calculated.

Statistical analysis

GraphPad Prism 9 was used for statistical analyses. Group differences were assessed and analyzed with a Kruskal-Wallis test, and post hoc comparison was done using the Mann-Whitney U test. $p<0.05$, indicates statistically significant.

Result

Micro-CT analysis of femurs in different rat groups

Figure 1A shows that the OVX group experienced a notable reduction in distal femoral trabeculae, marked by a sparse trabecular structure and reduced bone volume. The OVX+DH group confirmed substantial improvements in the number, structure, and integrity of trabeculae. Figure 1B-G suggests that the OVX group exhibited notably lower BV/TV, BS/BV, BS/TV, Tb.Th, and Tb.N. In contrast, the OVX+DH group demonstrated significant increases in BV/TV, Tb.Th, and Tb.N. These recommend that DH effectively mitigates the deterioration of trabecular microstructure and the development of osteoporosis in OVX rats.

Serum ELISA results

As shown in Fig. 1H-J, ALP, OPN, and OCN showed statistically significant differences between the OVX and Sham groups ($p<0.05$). Additionally, ALP and OPN exhibited statistically significant differences between the OVX and OVX+DH groups ($p<0.05$).

Results of histopathological analysis

HE staining and micro-CT analysis yielded consistent results (Fig. 2A). Both techniques demonstrated that in the Sham group, the trabeculae were dense, homogeneous, and continuous. In the OVX group, the trabeculae were reduced, fragmented, and sparsely arranged, with increased spacing and a significantly reduced area. In contrast, in the DH group, the bone trabeculae showed increased area and overall improvement. This may be attributed to the beneficial effect of DH on bone microarchitecture.

Immunohistochemical results

Figure 2B indicates a significantly higher count of TRAP-positive cells in the OVX relative to the sham($p<0.05$). Conversely, the DH exhibited a statistically sizeable reduction in osteoclast numbers compared to the OVX($p<0.05$), indicating that DH effectively inhibits osteoclastic bone resorption in rats. Figure 2C shows that OPN expression was significantly reduced in the

Table 1 The sequence of primers used in RT-qPCR

Gene name	Forward primer	Reverse primer
OCN	CTACCTGTATCAATGGCTGGG	GGATTGAGCTCACACACCT
OPN	TCACACATGGAAAGCGAGGAGTTG	ACTGTCCTTCCCACGGCTGTC
COL1A1	AAAGATGGACTCAACGGTCTC	CATCGTGAGCCTTCTCTTGAG
RUNX2	AGGCAGTTCCCAAGCATTTCATCC	TGGCAGGTAGGTGTGGTAGTGAG
OSX	ATAGTGGGCAGCTAGAAGGGAGTG	ATTAGGGCAGTCGCAGGAGGAG
CAT	GACATTACCAAATACTCCAAGGCAAAG	GAACCCGATTCTCCAGCAACAG
SOD1	GCCGTGTGCGTGCTGAAG	TTCACTGGTCCATTACTTTCCTTCTG
SOD2	GCACCACAGCAAGCACCAC	TGATATGACCACCACCATTGAACTTC
GAPDH	CAAGAGCACAAGAGGAAGAGAG	CTACATGGCAACTGTGAGGAG

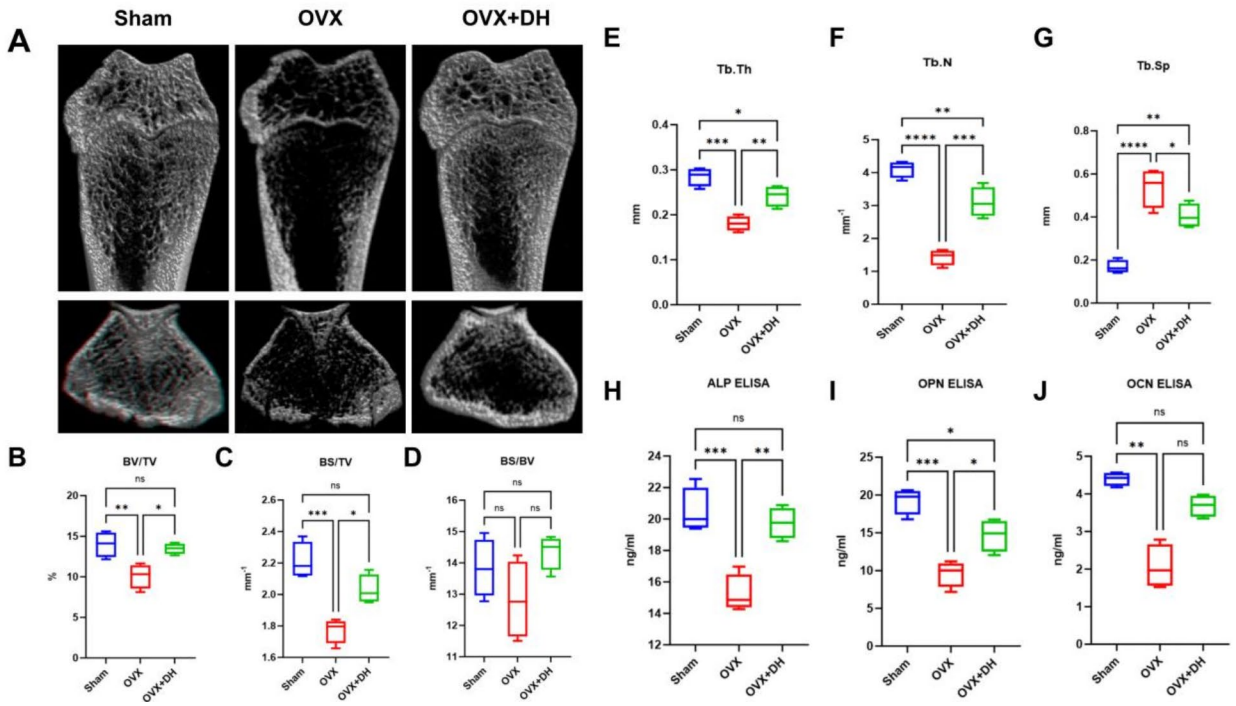

Fig. 1 Micro-CT pictures of femurs (**A**) and Micro-CT parameters, including BS/TV (**B**), BS/BV (**C**), BV/TV (**D**), Tb.Th (**E**), Tb.N (**F**), and Tb.Sp (**G**).Levels of serum ALP(**H**), OPN(**I**), and OCN(**J**) in three groups($n=4$)

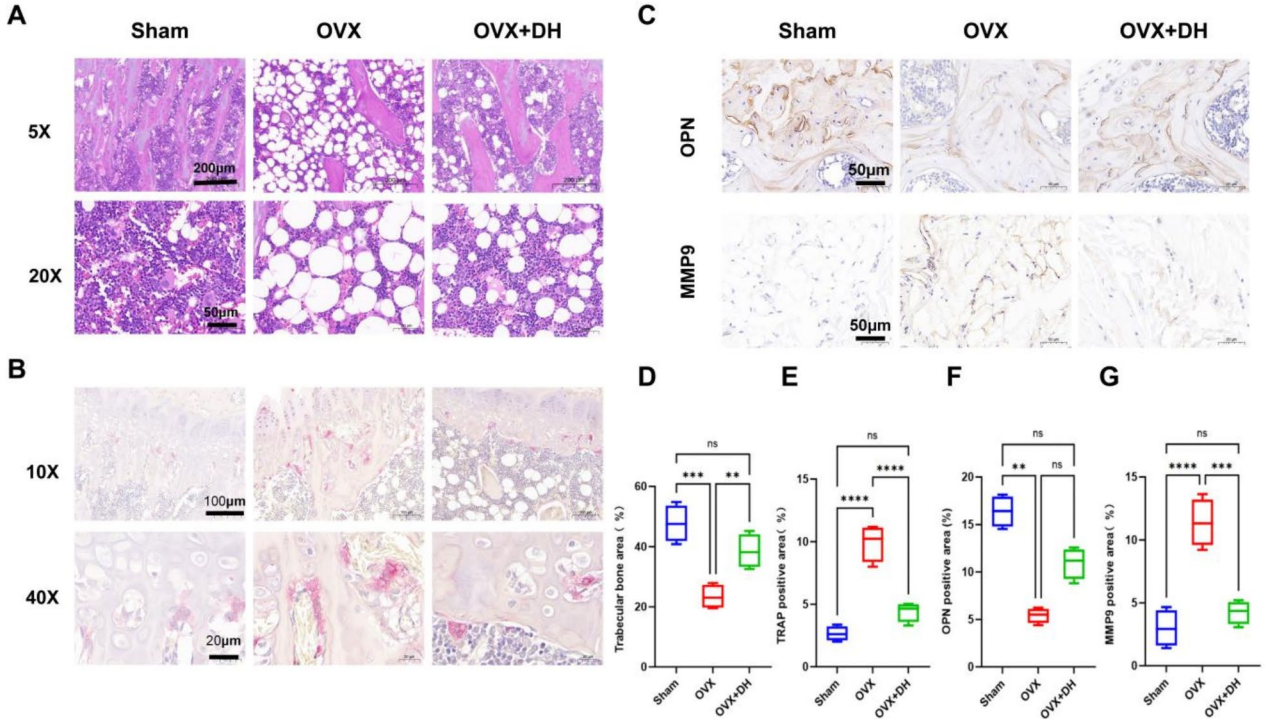

Fig. 2 HE staining (**A**), Immunohistochemical staining of TRAP(B), OPN (**C**), and MMP9 (**C**) in the tibia. D, E, F, and G display the statistical analysis results of HE staining (A), immunohistochemical staining of TRAP (**B**), OPN (**C**), and MMP9 (**D**), respectively

OVX group compared to the Sham group, with this difference reaching statistical significance($p<0.05$). No significant difference was observed between the other two groups($p>0.05$). Figure 2C shows that MMP9 expression was considerably greater in the OVX than in both the Sham and OVX+DH($p<0.05$). However, no significant difference was observed between the OVX+DH and Sham($p>0.05$). These findings suggest that DH treatment effectively reduced the expression of MMP9.

Results of cell proliferation experiments

As shown in Fig. 3A, both 1.0 μM and 1.5 μM concentrations of DH significantly promoted the proliferation of HS-5 cells, with differences compared to the control group reaching statistical significance ($p<0.05$). In contrast, 2.0 μM of DH inhibited the proliferation of HS-5 cells, and this inhibition was statistically significant relative to the control group ($p<0.05$).

Influences of DH on the osteogenic differentiation of HS-5

ALP staining and ALP activity results

DH at concentrations of 0.5–1.5 μM enhanced ALP activity compared to the control group (Fig. 3B).

Results of ARS Staining and quantitative analysis of mineralized nodules

ARS staining intensity increased progressively with 0.5–1.5 μM DH compared to the control group (Fig. 3C), and the quantitative analysis of mineralized nodules revealed statistically significant.

RT-qPCR results

Compared to the control group, a concentration of 0.5 μM increased the expression of COL1A1, RUNX2, OSX, OPN, and OCN genes, although the effect was not statistically significant ($p>0.05$). In contrast, 1.0 μM and 1.5 μM concentrations significantly upregulated the expression of these genes (Fig. 4A-E, $p<0.05$).

Western blot results

In line with the RT-qPCR results, 0.5 μM increased the protein expression of RUNX2, OPN, and OCN proteins, though this effect was not statistically significant ($p>0.05$). In contrast, 1.0 μM and 1.5 μM considerably expanded RUNX2, OPN, and OCN proteins (Fig. 4F, $p<0.05$).

Effects of DH on oxidative stress

Figure 5A shows that DCFH-DA expression was extensively higher in the H_2O_2 group compared to the control, but appreciably lower in the H_2O_2+DH group compared to the H_2O_2. RT-qPCR results indicated significantly reduced expression of CAT, SOD1, and SOD2 genes in the H_2O_2 group relative to the control($p<0.05$). While CAT, SOD1, and SOD2 gene expression levels were elevated in the H_2O_2+DH group compared to the H_2O_2 group (Fig. 5B-D, $p<0.05$). Western blot analysis revealed

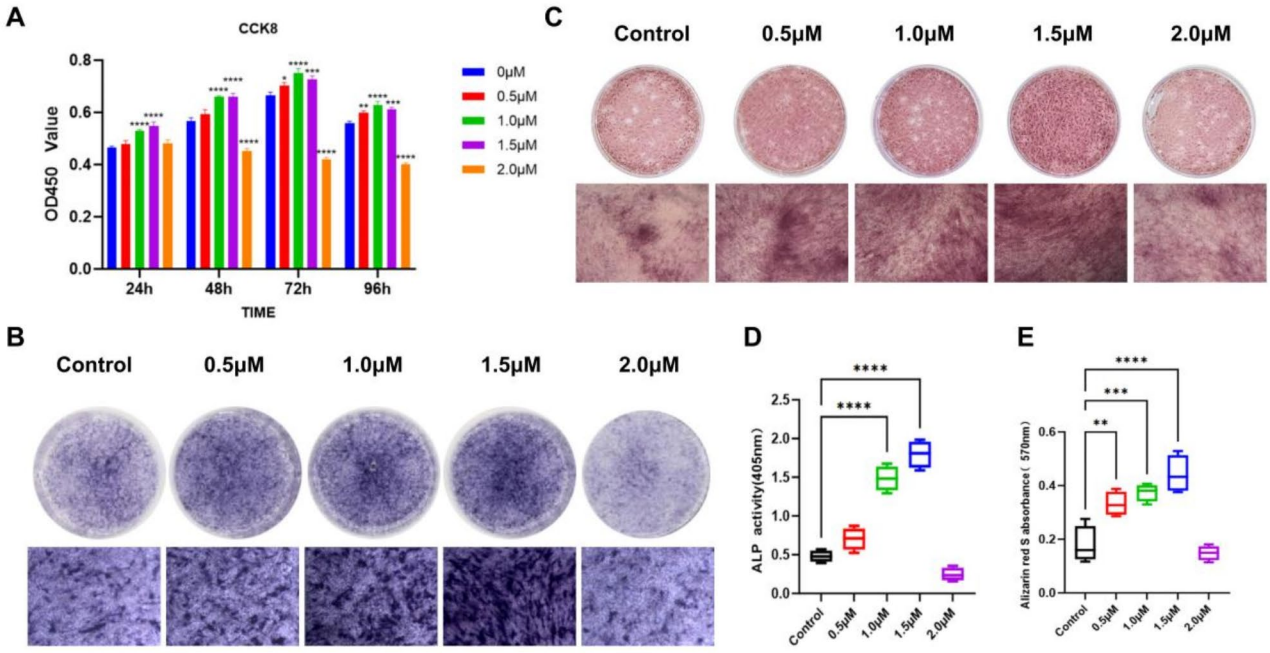

Fig. 3 Cell proliferation assay (**A**). ALP (**B**), ARS (**C**) staining, and statistical analysis (**D**, **E**) in three groups. The tests were carried out thrice

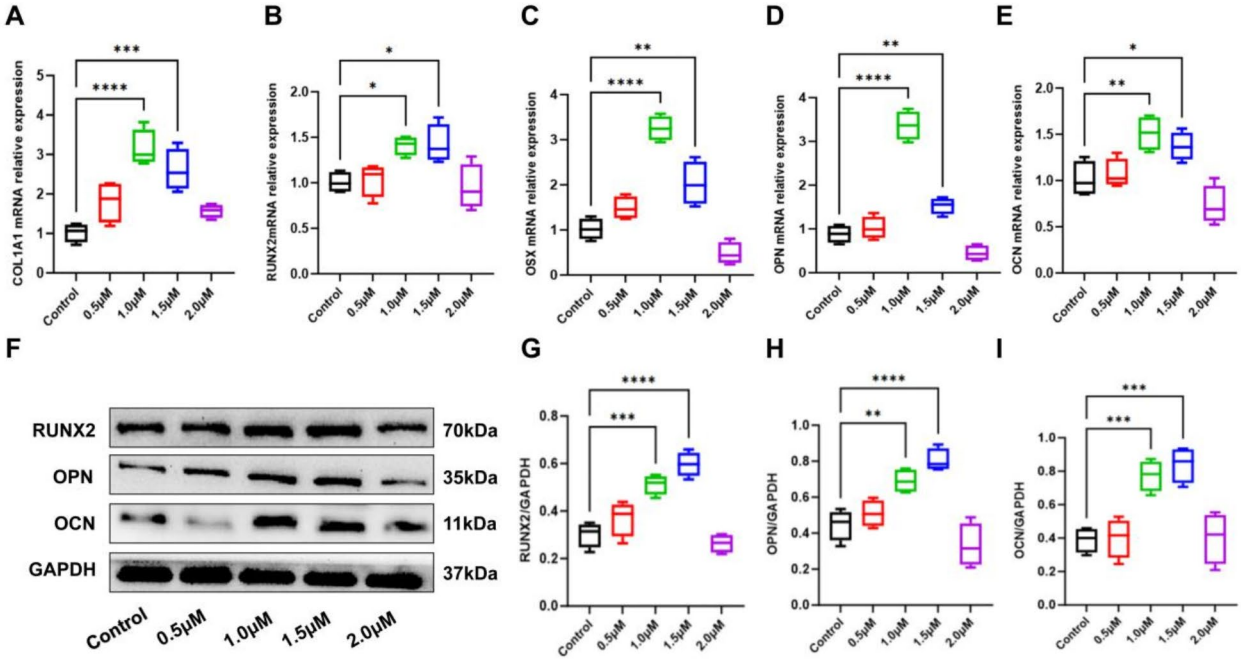

Fig. 4 RT-qPCR analysis of mRNA expression for COL1A1 (**A**), RUNX2 (**B**), OSX (**C**), OPN (**D**), and OCN (**E**) genes. Gene expression levels were normalized against GAPDH. Protein expression levels of RUNX2, OPN, and OCN(**F**) were analyzed using Western blotting. GAPDH served as the loading control. The protein levels of RUNX2(**G**), OPN(**H**), and OCN(**I**) were quantified using densitometric analysis and normalized to GAPDH. The experiment was conducted thrice

a significant decrease in SOD1 and SOD2 protein levels in the H_2O_2, whereas these levels substantially elevated in the H_2O_2+DH relative to the H_2O_2 group (Fig. 5E-G). The findings indicate that DH reduces intracellular oxidative stress.

DH promotes Osteogenesis by inhibiting oxidative stress

As depicted in Fig. 5H-K, the H_2O_2 group exhibited significantly reduced, ALP, and ARS staining, along with fewer ALP-active and mineralized nodules, compared to the control group($p<0.05$). These parameters were elevated in the H_2O_2+DH group compared to the H_2O_2 group ($p<0.05$).

Discussion

Osteoporosis, marked by increased bone turnover and decreased bone mass, occurs as a result of an imbalance between bone resorption and bone formation, main to skeletal fragility and a higher fracture risk [18, 19]. It represents a significant public health challenge, affecting approximately 200 million individuals worldwide, predominantly aged over 60 [20]. The increasing incidence of osteoporosis in our aging population highlights the urgent need for comprehensive studies to identify new therapeutic targets. We investigated the effects of DH on OVX rats and HS-5 cells, elucidating its mechanisms of action. Our findings indicate that DH may enhance osteoblast viability, promote osteoclast differentiation, and protect HS-5 cells from the effects of hydrogen peroxide-induced oxidative stress. However, it cannot be fully reduced, as the normal process of bone reconstruction relies on the production of a certain level of oxygen-free radicals [21].

Animal experiments using micro-CT and HE staining revealed that DH significantly improved the structure and quantity of bone trabeculae in OVX rats. Serum levels of ALP, OPN, and OCN were higher in the DH group in contrast to the OVX. The increased expression of OPN observed through immunohistochemistry was consistent with the ELISA results. DH treatment reduced TRAP-positive cells and immunohistochemical MMP9 expression. These findings indicate that DH enhances trabecular number and thickness, reduces trabecular separation, improves bone histology, and boosts osteogenic capacity in OVX rats, promoting bone formation, and inhibiting bone resorption by osteoclasts, thereby ameliorating osteoporosis.

In cellular experiments, we investigated the impact of DH on osteoblast proliferation and differentiation.ALP is an essential marker for early osteogenic differentiation and a vital enzyme in bone matrix formation [12]. OPN, primarily secreted by osteoblasts, is a phosphorylated

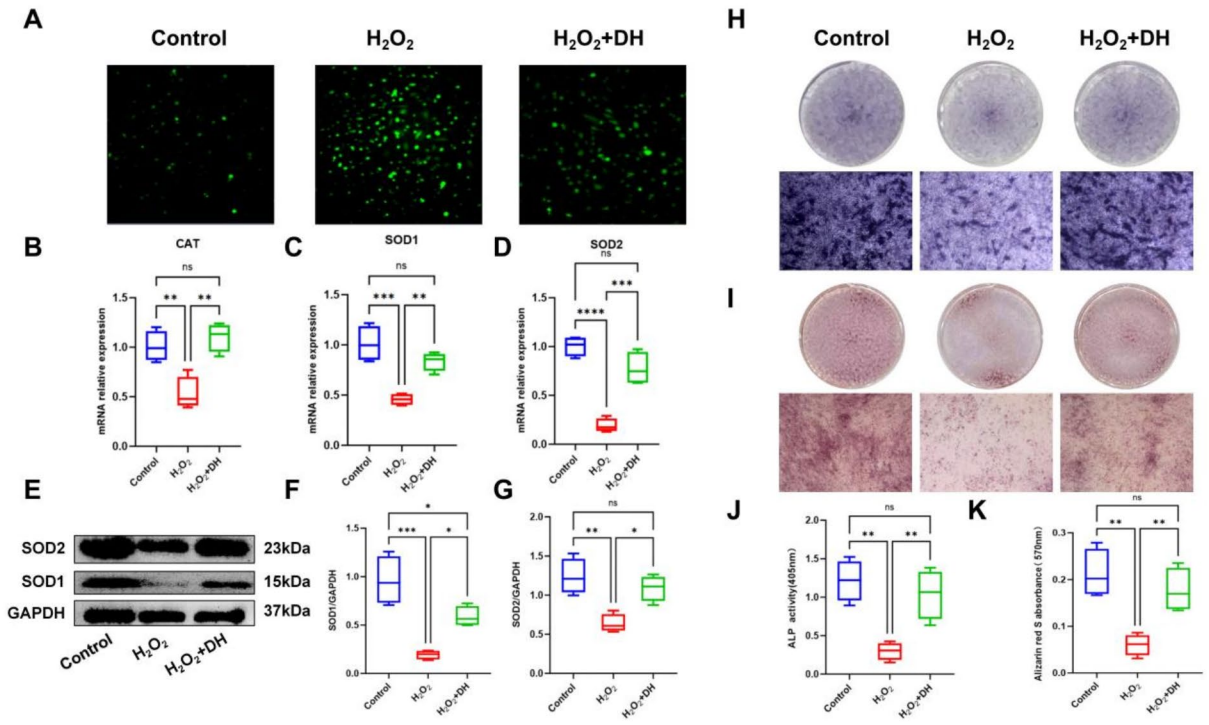

Fig. 5 Intracellular ROS levels in HS-5 cells (**A**). RT-qPCR analysis of CAT(**B**), SOD1(**C**), and SOD2(**D**) genes. Gene expression levels were normalized against GAPDH. Protein expression of SOD1 and SOD2 by Western Blot. Densitometric analysis was used to assess SOD1(**F**) and SOD2(**G**) protein levels, calculated as a ratio relative to GAPDH protein levels.ALP (**H**), ARS (**I**) staining and statistical analysis (**I**, **K**) in three groups. These experiments used to be performed thrice

protein associated with bone strength and remodeling and offers protection against osteoporosis [22, 23]. RUNX2, a transcription factor, is crucial for osteoinduction and bone tissue formation and remodeling [24, 25]. OCN, a non-collagenous bone matrix protein secreted and synthesized by osteoblasts, serves as a marker for mature osteoblasts and is vital for bone metabolism, including mineralization [26]. Thus, ALP staining, RT-qPCR, and Western Blot assays were utilized to evaluate ALP activity and the expression levels of OCN, OPN, and RUNX2 genes and proteins in osteoblasts. Results indicated that, after 7 days of intervention with varying DH concentrations, the highest ALP activity and protein expression levels for OCN, OPN, and RUNX2 were observed at 1.5μM.

Maintaining cellular redox homeostasis hinges on the dynamic stability between ROS manufacturing and antioxidant capacity [8]. Oxidative stress takes place when increased ROS exceeds cellular antioxidant defenses, leading to harm to nucleic acids, proteins, and lipids [27–29]. Organisms have developed antioxidant defense mechanisms, such as superoxide dismutase (SOD), catalase (CAT), glutathione peroxidase (GPX), glutathione reductase (GRX), thioredoxin (TXN), and peroxiredoxin (PRX), to mitigate oxidative cellular damage and maintain physiological ROS levels. These enzymes convert H_2O_2 into water H_2O [30]. Osteoporosis is traditionally attributed to factors involving hormonal changes, deficiencies in calcium and vitamin D, and the natural aging process. Oxidative stress has also emerged as a sizeable factor in literature [31–34]. Bai et al. discussed how H_2O_2-induced oxidative stress inhibits osteogenic differentiation in rabbit BMSCs and cranial osteoblasts [35]. Li et al. examined luteolin's role in preventing osteoporosis in rats by reducing oxidative stress and inhibiting osteoblast-specific protein expression [36]. Tao et al. investigated probucol, which was shown to enhance osteoblast activity and function in an ovariectomized rat model by promoting bone formation through reduced intracellular ROS levels [13]. Xu et al. reported that 4-MC prevents OVX-induced bone loss by inhibiting ROS production via Keap1 inhibition [37]. The antioxidant N-acetylcysteine (NAC) significantly enhances osteoblastic bone formation in OVX mice [38]. Additionally, melatonin, α-lipoic acid, and resveratrol have shown potential in promoting osteoblast differentiation and aiding in osteoporosis recovery through their antioxidant properties [39–41]. In our experiments, we observed that DH not only enhances osteoblast proliferation and differentiation but also markedly reduces intracellular ROS levels and promotes the expression of CAT, SOD1, and SOD2. These findings suggest that DH improves the intracellular oxidative stress

state by inhibiting ROS production, enhancing antioxidant expression, and promoting osteoblast differentiation by alleviating oxidative stress.

In conclusion, DH may improve osteoblast function and activity by inhibiting intracellular oxidative stress. This study suggests that DH may be a potential approach to ameliorate oxidative stress-related osteoporosis and other forms of osteoporosis, but more experimental validation of the specific efficacy is needed. As the treatment duration in this study was limited to 3 months, its long-term effects remain uncertain. In addition, due to the limited specificity and small number of rats, further studies are needed to determine whether DH is effective in all types of osteoporosis.

Supplementary Information

The online version contains supplementary material available at https://doi.org/10.1186/s13018-024-05398-0.

Supplementary Material 1

Acknowledgements
The authors express gratitude to the Zhejiang Provincial Natural Science Foundation.

Author contributions
Meichun Han: Conceptualization; Data curation; Formal Analysis; Software; Writing – Original Draft Preparation. Weibin Du: Data curation; Investigation. Lei Zhang: Investigation; Validation. Zhenwei Wang: Forrmal Analysis; Software. Shengqiang Fang: Formal Analysis; Resources. Yang Zheng: Project Administration; Visualization; Writing – Review & Editing. Renfu Quan: Funding Acquisition; Project Administration; Supervision.

Funding
This research was supported by the Zhejiang Natural Science Foundation (NO.TGY23H060013) and the Hangzhou Medical and Health Science and Technology Project (20220919Y085).

Data availability
No datasets were generated or analysed during the current study.

Declarations

Competing interests
The authors declare no competing interests.

Institutional Review Board Statement
The experimental protocol was approved by the Ethics Committee of Zhejiang Chinese Medical University (IACUC-20210517-05).

Received: 6 November 2024 / Accepted: 19 December 2024
Published online: 03 January 2025

References

1. Sambrook P, Cooper C. Osteoporos Lancet. 2006;367(9527):2010–8.
2. Sobh MM et al. Secondary osteoporosis and metabolic bone diseases. J Clin Med, 2022. 11(9).
3. Brown JP. Long-term treatment of postmenopausal osteoporosis. Endocrinol Metab (Seoul). 2021;36(3):544–52.
4. Maria S, Witt-Enderby PA. Melatonin effects on bone: potential use for the prevention and treatment for osteopenia, osteoporosis, and periodontal disease and for use in bone-grafting procedures. J Pineal Res. 2014;56(2):115–25.
5. Wang X, et al. Melatonin prevents bone destruction in mice with retinoic acid-induced osteoporosis. Mol Med. 2019;25(1):43.
6. Zhang C, et al. Oxidative stress: a common pathological state in a high-risk population for osteoporosis. Biomed Pharmacother. 2023;163:114834.
7. Bhatti JS, Bhatti GK, Reddy PH. Mitochondrial dysfunction and oxidative stress in metabolic disorders - A step towards mitochondria based therapeutic strategies. Biochim Biophys Acta Mol Basis Dis. 2017;1863(5):1066–77.
8. Valko M, et al. Free radicals and antioxidants in normal physiological functions and human disease. Int J Biochem Cell Biol. 2007;39(1):44–84.
9. Wauquier F, et al. Oxidative stress in bone remodelling and disease. Trends Mol Med. 2009;15(10):468–77.
10. López-Armada MJ, Fernández-Rodríguez JA, Blanco FJ. Mitochondrial dysfunction and oxidative stress in rheumatoid arthritis. Antioxid (Basel), 2022. 11(6).
11. Munmun F, Witt-Enderby PA. Melatonin effects on bone: implications for use as a therapy for managing bone loss. J Pineal Res. 2021;71(1):e12749.
12. Nakamura A, et al. Osteocalcin secretion as an early marker of in vitro osteogenic differentiation of rat mesenchymal stem cells. Tissue Eng Part C Methods. 2009;15(2):169–80.
13. Tao ZS, Li TL, Wei S. Probucol promotes osteoblasts differentiation and prevents osteoporosis development through reducing oxidative stress. Mol Med. 2022;28(1):75.
14. Zhang L, et al. Belamcanda chinensis (L.) DC-An ethnopharmacological, phytochemical and pharmacological review. J Ethnopharmacol. 2016;186:1–13.
15. Wen Y, et al. A novel strategy to evaluate the quality of herbal products based on the chemical profiling, efficacy evaluation and pharmacokinetics. J Pharm Biomed Anal. 2018;161:326–35.
16. Song YY et al. Phenolic compounds from Belamcanda chinensis seeds. Molecules, 2018. 23(3).
17. Woźniak D, Matkowski A. Belamcandae chinensis rhizome–a review of phytochemistry and bioactivity. Fitoterapia. 2015;107:1–14.
18. Tang CH. Osteoporosis: from Molecular mechanisms to therapies. Int J Mol Sci, 2020. 21(3).
19. Arceo-Mendoza RM, Camacho PM. Postmenopausal osteoporosis: latest guidelines. Endocrinol Metab Clin North Am. 2021;50(2):167–78.
20. Wright NC, et al. The recent prevalence of osteoporosis and low bone mass in the United States based on bone mineral density at the femoral neck or lumbar spine. J Bone Min Res. 2014;29(11):2520–6.
21. Almeida M, et al. Oxidative stress antagonizes wnt signaling in osteoblast precursors by diverting beta-catenin from T cell factor- to forkhead box O-mediated transcription. J Biol Chem. 2007;282(37):27298–305.
22. Bai RJ, Li YS, Zhang FJ. Osteopontin, a bridge links osteoarthritis and osteoporosis. Front Endocrinol (Lausanne). 2022;13:1012508.
23. Si J, et al. Osteopontin in Bone Metabolism and Bone diseases. Med Sci Monit. 2020;26:e919159.
24. Farrokhi E, et al. Effect of oxidized low density lipoprotein on the expression of Runx2 and SPARC genes in vascular smooth muscle cells. Iran Biomed J. 2015;19(3):160–4.
25. Yu Y, et al. Knockdown of lncRNA KCNQ1OT1 suppresses the adipogenic and osteogenic differentiation of tendon stem cell via downregulating miR-138 target genes PPARγ and RUNX2. Cell Cycle. 2018;17(19–20):2374–85.
26. Liu Z, et al. DNA demethylation rescues the impaired osteogenic differentiation ability of Human Periodontal Ligament Stem cells in high glucose. Sci Rep. 2016;6:27447.
27. Ray PD, Huang BW, Tsuji Y. Reactive oxygen species (ROS) homeostasis and redox regulation in cellular signaling. Cell Signal. 2012;24(5):981–90.
28. Schieber M, Chandel NS. ROS function in redox signaling and oxidative stress. Curr Biol. 2014;24(10):R453–62.
29. Demir Y, Balcı N, Gürbüz M. Differential effects of selective serotonin reuptake inhibitors on paraoxonase-1 enzyme activity: an in vitro study. Comp Biochem Physiol C Toxicol Pharmacol. 2019;226:108608.
30. Liu M et al. Insights into Manganese Superoxide Dismutase and Human diseases. Int J Mol Sci, 2022. 23(24).
31. Manolagas SC. The Quest for osteoporosis mechanisms and rational therapies: how far we've come, how much further we need to go. J Bone Min Res. 2018;33(3):371–85.
32. Domazetovic V, et al. Oxidative stress in bone remodeling: role of antioxidants. Clin Cases Min Bone Metab. 2017;14(2):209–16.
33. Banfi G, Iorio EL, Corsi MM. Oxidative stress, free radicals and bone remodeling. Clin Chem Lab Med. 2008;46(11):1550–5.

34. Baek KH, et al. Association of oxidative stress with postmenopausal osteoporosis and the effects of hydrogen peroxide on osteoclast formation in human bone marrow cell cultures. Calcif Tissue Int. 2010;87(3):226–35.
35. Bai XC, et al. Oxidative stress inhibits osteoblastic differentiation of bone cells by ERK and NF-kappaB. Biochem Biophys Res Commun. 2004;314(1):197–207.
36. Li H, et al. Lutein suppresses oxidative stress and inflammation by Nrf2 activation in an osteoporosis rat model. Med Sci Monit. 2018;24:5071–5.
37. Xu Y, et al. Pharmacology-based molecular docking of 4-methylcatechol and its role in RANKL-mediated ROS/Keap1/Nrf2 signalling axis and osteoclastogenesis. Biomed Pharmacother. 2023;159:114101.
38. Shi C, et al. Bone marrow ablation demonstrates that estrogen plays an important role in osteogenesis and bone turnover via an antioxidative mechanism. Bone. 2015;79:94–104.
39. Chen W et al. *Melatonin Improves the Resistance of Oxidative Stress-Induced Cellular Senescence in Osteoporotic Bone Marrow Mesenchymal Stem Cells.* Oxid Med Cell Longev, 2022;7420726.
40. Liu X, et al. Resveratrol induces proliferation in preosteoblast cell MC3T3-E1 via GATA-1 activating autophagy. Acta Biochim Biophys Sin (Shanghai). 2021;53(11):1495–504.
41. Lu SY, et al. The osteogenesis-promoting effects of alpha-lipoic acid against glucocorticoid-induced osteoporosis through the NOX4, NF-kappaB, JNK and PI3K/AKT pathways. Sci Rep. 2017;7(1):3331.

Publisher's note